# Nonlinear Domain-Wall Velocity Enhancement by Spin-Polarized Electric Current

G. S. D. Beach,* C. Knutson, C. Nistor, M. Tsoi, and J. L. Erskine
*Department of Physics, The University of Texas at Austin, Austin, Texas 78712-0264, USA*
(Received 24 February 2006; published 4 August 2006)

The interaction between a dc spin-polarized electric current and a magnetic domain wall in a Permalloy nanowire was studied by high-bandwidth scanning Kerr polarimetry. The full functional dependence of wall velocity on electric current and magnetic field is presented. With the pinning potential nulled by a field, current-induced velocity enhancements exceeded 35 m/s at a current density of $\sim 6 \times 10^{11}$ A/m$^2$. This large enhancement, more than 10 times that found in pinning-dominated experiments, results in part from an interaction that is nonlinear in current and independent of current direction.

DOI: 10.1103/PhysRevLett.97.057203 PACS numbers: 75.60.Ch, 75.75.+a, 85.75.−d

The domain walls separating regions of opposing magnetization in a ferromagnet may be manipulated not only by a magnetic field, but also by an electric current [1–11], most notably through the mechanisms of the spin-torque interaction [2,12–17]. As a spin-polarized electron passes through a domain wall, its spin direction follows the local magnetization and rotates from the spin ''up'' state to spin ''down''. The quantum $\hbar$ of angular momentum involved in this rotation must be conserved, and is consequently transferred to the spins within the wall. The transfer of momentum exerts a torque on the wall magnetization and may apply a force to the wall that acts much like a pressure applied to a macroscopic object. Recent demonstrations that this ''spin pressure'' can be great enough to move a domain wall [3–11] have spurred extensive research, in large part because of its potential impact in spintronic device technology [6–9].

Many recent experiments have focused on current-induced depinning of a domain wall from material defects or engineered pinning sites [7–9], but few have addressed the subsequent propagation of a depinned wall. Existing observations of current-driven wall propagation [10,11] find velocities one or 2 orders of magnitude less than those predicted by theory [12–17]. This discrepancy suggests that in real devices, most of the transferred momentum is dissipated by local excitations [10] rather than being used to drive wall motion. If current-driven domain-wall motion were really this inefficient, it would have serious consequences on the ultimate viability of spin-torque in applications: the maximum velocities of current-driven walls would be quite low, and the current densities required to achieve even those velocities would dissipate too much energy to be practical.

In this Letter we use an external field to null extrinsic pinning and identify the contribution of spin torque to the terminal velocity $v$ of a freely-propagating domain wall. We find current is far more efficient at translating a wall than pinning-dominated experiments suggest. We also evaluate the response of $v$ to field and current over ranges broad enough to discern its functional form and make meaningful comparisons with theory. We find that $v$ is enhanced in proportion to current by an amount in accord with recent predictions [15,17]. We also uncover a further augmentation of $v$ by a heretofore-unrealized interaction that is nonlinear in current and independent of its direction relative to $v$.

Experiments were performed using the nanowire geometry shown in Fig. 1(a). A 20 nm-thick $Ni_{80}Fe_{20}$ film, grown on and capped by Ta layers of thickness 5 nm and 3 nm, respectively, was sputter deposited on a thermally oxidized Si substrate. The film was milled with a focused $Ga^+$ beam to form a 600 nm by 40 $\mu$m nanowire. The wire joined two large-area film regions otherwise electrically

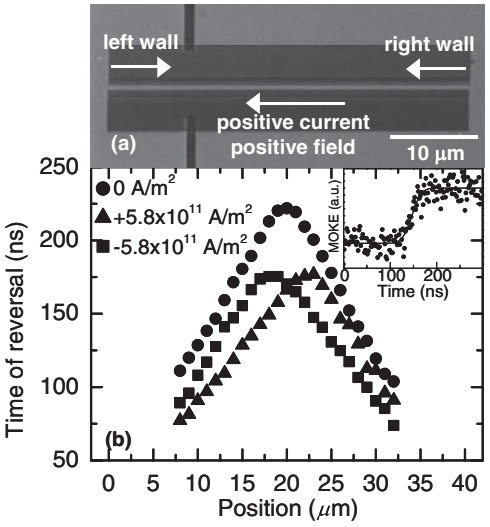


FIG. 1. (a) Scanning electron micrograph of nanowire and contiguous large-area film regions (light contrast) and milled regions (dark contrast). Directions of domain-wall propagation, positive applied field, and positive current (opposite to direction of $e^-$ flow) are indicated by arrows. (b) Inset shows time-resolved magneto-optic Kerr effect measured 12 $\mu$m from the left film-nanowire junction for $H = 46$ Oe and $j = 0$. The temporal centers of reversal transients are plotted versus position for $j = 0$ and $j = \pm 5.8 \times 10^{11}$ A/m$^2$ ($t = 0$ when field step crosses the injection field).

 

isolated from each other by a milled trench. The large-area regions served as current-injection pads and as domain-wall nucleation sources. Magnetic reversal was effected by applying a negative saturating field followed by a positive field step [18] along the wire axis, nucleating domain walls in the film and driving them simultaneously into each end of the wire and towards its center.

Time-resolved domain-wall propagation was studied using high-bandwidth scanning Kerr polarimetry, closely following the approach of Ref. [19]. Mean wall arrival times at fixed positions along the wire were determined from the time-resolved Kerr rotation [Fig. 1(b), inset] probed with a 2.5 $\mu$m laser spot and averaged over $3 \times 10^4$ reversal cycles. Results are shown in Fig. 1(b) for $H = 46$ Oe with current densities $j = 0$ and $\pm 5.8 \times 10^{11}$ A/m$^2$. Reversal proceeds along the wire with a progressive delay increasing linearly with distance from the film-nanowire junctions, confirming wall propagation. The narrow temporal widths of the (averaged) reversal transients and the sharply defined position of left-right wall annihilation [central cusp in Fig. 1(b)] indicate that the process is highly repetitive from cycle to cycle [19].

The average velocity $v$ of each wall, taken as positive for motion towards the wire center, was obtained from the inverse slope of its trajectory. At $j = 0$ the left and right walls in Fig. 1(b) travel with nearly the same velocity, and meet near the center of the nanowire. When a positive current is applied, the velocity of the left wall, which travels with the electron flow, increases from 97 m/s to 132 m/s, and it travels several micrometers past the nanowire center before meeting the slower right wall. The trajectories are reversed for negative-current polarity. The large velocity enhancement of $\sim$35 m/s observed here for wall motion parallel to the electron flow is far in excess of the 0.2–2 m/s reported in pinning-dominated experiments [10,11], and much closer to theoretical expectations. However, rather than a corresponding reduction in the velocity of a wall moving against the spin current, the data show a small *increase* in wall velocity. Thus it appears the net influence of current is more complex than existing models predict.

Two forms of spin-transfer torque have so far been proposed: adiabatic [12–14,16,20] and nonadiabatic [2,12,15,17]. When a domain wall is wide, the electron spin can adiabatically follow the slowly varying local spin direction as it traverses the wall. As the electron spin rotates, it exerts a torque on the wall normal to its plane of magnetization. If the spatial gradient in local magnetization across the wall is too large, a finite mistracking angle may develop between the electron spin and the local spins. This can result in spin-flip scattering of the electrons and a nonadiabatic pressure on the wall. For a domain wall of finite width, both effects should be expected in some proportion.

These two processes affect wall velocity in very different ways. Adiabatic torque cants the wall magnetization relative to the easy plane, changing the wall width $\Delta$ due to a change in magnetostatic energy. However, adiabatic torque is incapable of driving sustained wall motion, except at very large $j$ [13,14,16]. Instead, its effect on wall velocity is indirect. Under the action of a field $H$, a domain wall has in general a velocity $v = \mu_H(H - H_0)$ where the mobility $\mu_H$ is proportional to the effective wall width [21–23], and $H_0$ is a phenomenological "dynamic coercive field" [21]. By changing $\mu_H$, current can change the velocity of a wall under a given field, but it is the *field* that drives wall motion. At zero field, no current-driven terminal velocity is expected [13,14,16].

Nonadiabatic spin-transfer torque, by contrast, enters the domain-wall equations of motion as an effective field that applies a "pressure" directly to the wall [12,15,17]. This pressure augments $v$ by a field-independent amount $\mu_j j$ [15,17], with $\mu_j$ described below. Combined, these two processes lead to an expected domain-wall velocity of the form $v(H, j) = \mu_H(j)(H - H_0) + \mu_j j$. Nonadiabatic spin-transfer torque displaces the wall mobility curve $v(H, j)$, whereas adiabatic torque distorts it. A proper account of the spin-torque interaction evidently requires the full functional form of $v(H, j)$.

Figure 2 shows $v$ versus $H$ measured at $j = 0$ and $j = \pm 5.8 \times 10^{11}$ A/m$^2$. These curves exhibit two linear regimes, at low ($H < 6$ Oe) and high fields ($H > 35$ Oe), respectively, separated by a nonlinear regime at moderate $H$. This behavior results from Walker breakdown [21], recently observed in a similar nanowire as described in detail in Ref. [19]. Below the breakdown field $H_W = 6$ Oe, the wall propagates smoothly and its structure is preserved with time. Above $H_W$ the wall structure becomes unstable causing its instantaneous velocity to oscillate and its average velocity to drop abruptly. The oscillation frequency increases with increasing $H$, and its amplitude decreases, until $v(H)$ finally regains linearity but with a substantially lower mobility [21]. The $j = 0$ mobility curve exhibits a "hump" between 10 and 35 Oe that was not observed in

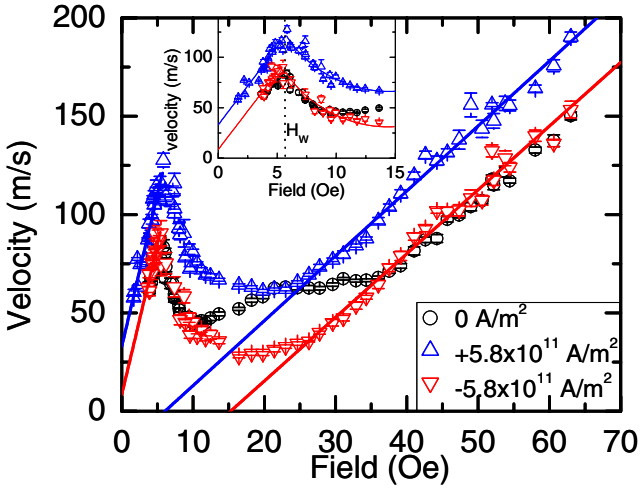


FIG. 2 (color online). Mobility curves for the left wall measured at $j = 0$ and $j = \pm 5.8 \times 10^{11}$ A/m$^2$.

Ref. [19]. The hump is suppressed by a current of either polarity. The origin of this hump is currently under investigation, and appears to be related to an increase in edge roughness due to a variation in the milling process.

With the exception of the turbulent intermediate-$H$ regime, $j$ simply imparts a vertical displacement to $v(H)$; i.e., $v$ at low and high $H$ is the sum of two *independent* terms, $v(H, j) = \mu_H(H - H_0) + \tilde{v}(j)$. Current does not significantly change the low- and high-field $\mu_H$ (and hence the effective wall width $\Delta$). This result is in accord with analytical [13,15] and micromagnetic [16,17] models that predict no change to $\mu_H$ by nonadiabatic torque and a negligible change by adiabatic torque at these currents. In addition, $H_W$ varies by no more than $\sim$0.5 Oe at the currents studied. In the micromagnetic simulations of Ref. [16], adiabatic torque shifted $H_W$ by only $\sim$10% at comparable current densities, within the range of experimental uncertainty. Although corresponding theoretical results for nonadiabatic torque have not been presented, Fig. 2 puts an experimental upper limit of $\sim$10% on its effect on $H_W$.

The lack of a symmetric vertical shift of the positive and negative-current $v(H)$ about the zero-current curve in Fig. 2 implies $v$ is not linear in $j$. In Fig. 3, $v(j)$ is plotted for several $H$. At intermediate fields, $v(j)$ exhibits several local maxima and minima, as the shape of the mobility curve changes qualitatively. In the low- and high-$H$ linear-mobility regimes, the form of $v(j)$ is independent of $H$ and exhibits a skewed quadratic character, with the velocities of both walls enhanced at large $|j|$.

The nearly field-independent behavior of $v(j)$ at low and high $H$ is suggestive of nonadiabatic spin-torque, but its functional form is unexpectedly complex. Interpretation of $v(j)$ is aided by considering its symmetric ($v_+$) and antisymmetric ($v_-$) components, $v_\pm(j) = [v(+j) \pm v(-j)]/2$. Figure 4 shows these components derived from the data of Fig. 3. $v_-$ is approximately linear for all $H$ and has the same slope but opposite sign for the left and right walls. The nonlinearity in $v(j)$ is contained in $v_+$. This component varies approximately as $j^2$ and augments the velocity of both walls, except at intermediate fields, where its sign inverts.

The antisymmetric component $v_-(j)$ is linear in $j$ and nearly independent of field, as seen in Fig. 4(g), even in the highly turbulent intermediate-field regime. Accordingly, we compare this term to theoretical models of nonadiabatic spin-transfer torque, from which these characteristics are expected. Nonadiabatic torque is predicted to augment $v$ by an amount [15,17] $\mu_j j$ with $\mu_j = (p\mu_B/eM_s\alpha)\beta$. Here, $p$ is the spin polarization of conduction electrons,

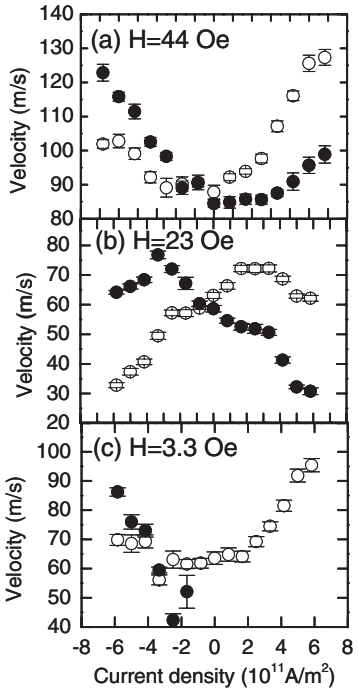


FIG. 3. Velocities of the left (open symbols) and right (solid symbols) domain walls as a function of current density for several field step amplitudes. At the lowest field, the right wall is pinned and does not propagate for positive currents.

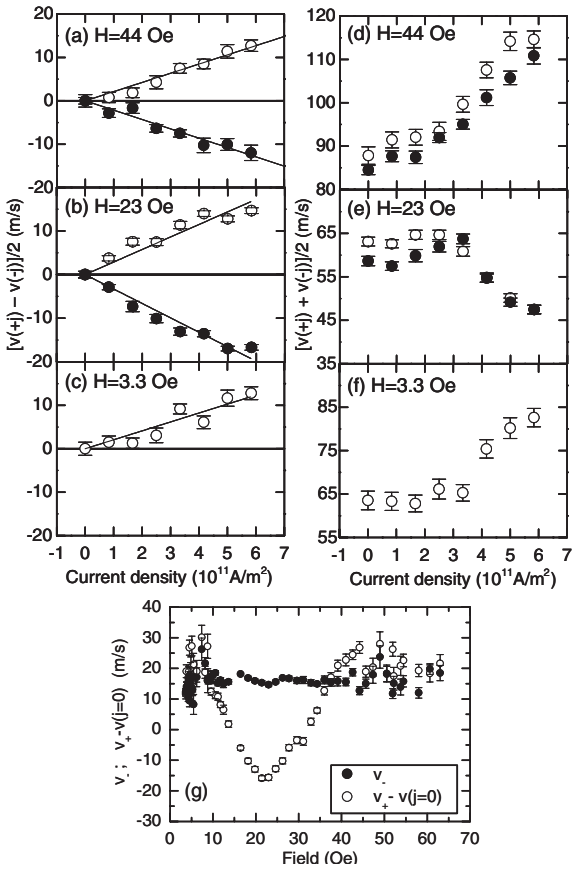


FIG. 4. (a), (b), (c) Antisymmetric ($v_-$) and (d), (e), (f) symmetric ($v_+$) velocity components of the left (open symbols) and right (solid symbols) walls versus current density for several fields. (g) $v_-$ and $v_+$ (with zero-current velocity offset subtracted) versus field for $|j| = 5.8 \times 10^{11}$ A/m$^2$.

$M_s$ the saturation magnetization, $\alpha$ the Gilbert damping, $\mu_B$ the Bohr magneton, and $e$ the electron charge. $\beta$ characterizes the strength of the nonadiabatic torque [17] and has been estimated [15,17] from the ratio of $\tau_{ex} = \hbar/J_{ex}$ to the spin-flip relaxation time ($J_{ex}$ is the exchange constant) to be of the order $10^{-2}$. Using parameters typical of $Ni_{80}Fe_{20}$ ($M_s = 790$ emu/cm$^3$, $\alpha \sim 0.01$, and $p \sim 0.5$) the average slope of $v_-(j)$, $\sim 2.7 \times 10^{-11}$ m$^3$/C, implies $\beta \sim 0.007$. The component $v_-(j)$ is thus qualitatively and quantitatively consistent with nonadiabatic spin torque.

To compare with other experiments, we define a model-independent efficiency $\varepsilon$ as the number of spins flipped in the ferromagnet (as the wall travels with velocity $v$) per conduction electron traversing the wall. In $Ni_{80}Fe_{20}$, the average moment per spin is $1.0\mu_B$ and hence an electron flips a spin in the ferromagnet with efficiency $\varepsilon = (2M_s e/\mu_B)\Delta v/j$, where $\Delta v$ is the current-induced change in $v$. The linear component $v_-$ drives the wall with a field-independent efficiency $\sim 0.7$ flipped spins per electron; the nonlinear component can increase $\varepsilon$ to $\sim 1.6$. By contrast, prior measures of current-only-driven wall motion in $Ni_{80}Fe_{20}$ had efficiencies, as defined here, of $\sim 0.1$ (Ref. [10]) and $\sim 0.04$ (Ref. [11]). In those experiments, the currents were at most $\sim 10\%$ larger than the average depinning threshold. Hence much of the transferred angular momentum was likely dissipated in overcoming local pinning, leading to an artificially low estimate of $\varepsilon$. When the pinning potential is offset by even a very small applied field, the intrinsic efficiency of the spin-torque interaction is seen to be much higher.

Although $v_-$ is well-described by existing theory, $v_+$ does not emerge directly from present models. As $v_+$ has the same form at low and high $H$, it is not due to the oscillatory wall dynamics above breakdown. Most spin-torque models assume a simple transverse domain wall. In nanowires of the present dimensions, the wall is more complex [23,24], with the in-plane magnetization circulating about a perpendicular "vortex core." It is unclear to what extent the simplified spin-torque models apply to such "vortex walls". Experiments have shown that current can act directly on a vortex (or Bloch line) within a wall, displacing it laterally along an extended wall [25], or toward the edge in a wire [11]. Because a vortex experiences a gyrotropic force transverse to its velocity [21], current-driven lateral displacement of a vortex within a wall yields a force on the wall parallel to the spin current [26]. In Ref. [11], current was able to transform a vortex wall in a nanowire into a transverse wall by driving the vortex out the edge of the wire. If current were likewise able to nucleate vortices, situations could arise to explain a symmetric velocity component. For example, if the nucleation probability were higher for electron flow in the direction of wall motion, then it would be more efficient for a spin current to speed up a moving wall than to slow it down, as observed in these experiments. Models with more realistic spin structures must be explored to determine if known spin-torque terms can account for our data, or whether additional sources of current-induced wall motion must be considered.

This work was supported by the NSF NIRT program (No. DMR-0404252) and R. A. Welch Foundation (No. F-1015). Instrumentation was developed with support from the NSF IMR program (No. DMR-0216726) and the Texas Coordinating Board (No. ATP-0099). Nanowires were fabricated using facilities of the Center for Nano and Molecular Science and Technology at UT Austin.

*Electronic address: gbeach@physics.utexas.edu

[1] L. Berger, Phys. Lett. A **46**, 3 (1973).
[2] L. Berger, J. Appl. Phys. **55**, 1954 (1984).
[3] P. P. Freitas and L. Berger, J. Appl. Phys. **57**, 1266 (1985).
[4] C. Y. Hung and L. Berger, J. Appl. Phys. **63**, 4276 (1988).
[5] L. Gan, S. H. Chung, K. H. Aschenbach, M. Dreyer, and R. D. Gomez, IEEE Trans. Magn. **36**, 3047 (2000).
[6] H. Koo, C. Krafft, and R. D. Gomez, Appl. Phys. Lett. **81**, 862 (2002).
[7] M. Klaui *et al.*, Appl. Phys. Lett. **83**, 105 (2003).
[8] M. Tsoi, R. E. Fontana, and S. S. P. Parkin, Appl. Phys. Lett. **83**, 2617 (2003).
[9] N. Vernier, D. A. Allwood, D. Atkinson, M. D. Cooke, and R. P. Cowburn, Europhys. Lett. **65**, 526 (2004).
[10] A. Yamaguchi *et al.*, Phys. Rev. Lett. **92**, 077205 (2004).
[11] M. Klaui *et al.*, Phys. Rev. Lett. **95**, 026601 (2005).
[12] G. Tatara and H. Kohno, Phys. Rev. Lett. **92**, 086601 (2004).
[13] Z. Li and S. Zhang, Phys. Rev. Lett. **92**, 207203 (2004).
[14] Z. Li and S. Zhang, Phys. Rev. B **70**, 024417 (2004).
[15] S. Zhang and Z. Li, Phys. Rev. Lett. **93**, 127204 (2004).
[16] A. Thiaville, J. Miltat, and J. Vernier, J. Appl. Phys. **95**, 7049 (2004).
[17] A. Thiaville, Y. Nakatani, J. Miltat, and Y. Suzuki, Europhys. Lett. **69**, 990 (2005).
[18] Fields were generated with a high-bandwidth magnet system with risetime $\sim 20$ ns. Fields greater than $H_i = 30$ Oe were required to inject a nucleated wall into the nanowire. For measurements below $H_i$, a short "injection pulse" (Ref. [19]) was first applied to inject a wall several micrometers into the wire. The addition of similar injection pulses prior to simple field steps above 30 Oe did not affect the terminal wall velocity.
[19] G. S. D. Beach, C. Nistor, C. Knutson, M. Tsoi, and J. L. Erskine, Nat. Mater. **4**, 741 (2005).
[20] L. Berger, J. Appl. Phys. **49**, 2156 (1978).
[21] A. P. Malozemo and J. C. Slonczewski, *Magnetic Domain Walls in Bubble Materials* (Academic Press, New York, 1979).
[22] A. Thiele, Phys. Rev. Lett. **30**, 230 (1973).
[23] Y. Nakatani, A. Thiaville, and J. Miltat, J. Magn. Magn. Mater. **290**, 750 (2005).
[24] R. D. McMichael and M. J. Donahue, IEEE Trans. Magn. **33**, 4167 (1997).
[25] C.-Y. Hung, L. Berger, and C. Y. Shih, J. Appl. Phys. **67**, 5941 (1990).
[26] L. Berger, J. Appl. Phys. **63**, 1663 (1988).